

Infrared Spectroscopic and Density Functional Theory Studies on the Reactions of Cadmium Atoms with Carbon Monoxide in Solid Argon

Ling Jiang and Qiang Xu*

National Institute of Advanced Industrial Science and Technology (AIST), Ikeda, Osaka 563-8577, and Graduate School of Science and Technology, Kobe University, Nada Ku, Kobe, Hyogo 657-8501, Japan

Received: June 25, 2005; In Final Form: August 2, 2005

Reactions of laser-ablated cadmium atoms with carbon monoxide molecules in solid argon have been investigated using matrix isolation infrared spectroscopy. On the basis of isotopic substitution, the absorption at 1858.2 cm^{-1} is assigned to the C–O stretching of the CdCO molecule, which is formed during the sample deposition. Cadmium di- and tricarbonyls, $\text{Cd}(\text{CO})_n$ ($n = 2, 3$), have not been observed under the same experimental conditions. Density functional theory calculations have been performed on the cadmium carbonyls $\text{Cd}(\text{CO})_n$ ($n = 1-3$), which lend strong support to the experimental assignments of the infrared spectra. It is predicted that the CdCO molecule is a linear triplet molecule and its formation involves Cd $5s \rightarrow 5p$ promotion. This promotion increases the Cd–CO bonding by decreasing the σ repulsion and increasing the Cd $5p$ orbital \rightarrow CO π^* back-donation. The absence of cadmium di- and tricarbonyls, $\text{Cd}(\text{CO})_n$ ($n = 2, 3$), has also been discussed in some detail.

Introduction

The interaction of carbon monoxide with metal atoms is of considerable interest from an academic and an industrial viewpoint.¹ Coordinatively unsaturated metal carbonyls are building blocks of stable organometallic complexes and can be exceedingly reactive and engage in a wide variety of chemical processes. Moreover, metal carbonyls are often considered as models for CO binding to the metal surface, which play important roles in catalysis and synthesis and as a moiety in the formation of long-lived complexes in the gas phase.¹⁻³ It is generally accepted that the bonding scheme of transition-metal carbonyls involves a σ -type dative interaction between the lone-pair electrons of CO and the vacant orbitals of the metal atom and π -type back-donation from the filled d_π orbitals of the metal atom to the vacant π^* orbitals of CO molecules.^{1,2} The bonding in the group 11 carbonyls is quite different from that in other transition-metal carbonyls,³⁻⁵ in part due to the extra stability of the completed nd^{10} configuration of the metal. It has been found that the $d_\pi \rightarrow \pi^*$ donation is primarily responsible for the formation of CuCO. The increased stability of the valence d orbital level for the second transition row dramatically increases the separation between the Ag d_π and CO π^* levels and therefore reduces the Ag $4d$ to CO π^* donation relative to that of CuCO. With neither CO σ donation to the metal nor metal to CO π^* donation, it is not surprising that AgCO is not formed. In the case of AuCO, the metal d_π of Au is between Cu and Ag and both σ and π donations are primarily responsible for its thermal stability.

With the completed $(n-1)d^{10}ns^2$ configuration of the group 12 metals, it is generally accepted that the 1S ground state is distinctively passive. However, the recently reported zinc tricarbonyl, $\text{Zn}(\text{CO})_3$, the next member of the series of 18-electron metal carbonyls, $\text{Cr}(\text{CO})_6 \rightarrow \text{Fe}(\text{CO})_5 \rightarrow \text{Ni}(\text{CO})_4$, offers a rare example of the reaction of Zn atoms with CO.⁶ It

has been found that the formation of $\text{Zn}(\text{CO})_3$ involves $4s \rightarrow 4p$ promotion of the Zn atom, which increases the Zn–CO bonding by decreasing the σ repulsion and significantly increasing the Zn $4sp$ hybrid orbitals \rightarrow CO π^* back-donation. However, the formation of zinc mono- and dicarbonyls, $\text{Zn}(\text{CO})_n$ ($n = 1, 2$), was absent from the previous investigations.

Recent studies have shown that, with the aid of isotopic substitution, matrix isolation infrared spectroscopy combined with quantum chemical calculation is very powerful in investigating the spectrum, structure, and bonding of novel species.^{3,6-8} In contrast with extensive experimental and theoretical studies of the interactions of CO molecules with the transition-metal and main-group-element atoms,^{3,6-8} however, almost nothing is known about a simple cadmium carbonyl molecule. Here we report a study of the reactions of laser-ablated cadmium atoms with CO molecules in excess argon. IR spectroscopy coupled with theoretical calculations provides evidence for the formation of a novel cadmium monocarbonyl, CdCO, whereas there is no evidence for the formation of the cadmium di- and tricarbonyls, $\text{Cd}(\text{CO})_n$ ($n = 2, 3$), in contrast with the case of $\text{Zn}(\text{CO})_n$ ($n = 1-3$).

Experimental and Theoretical Methods

The experiment for laser ablation and matrix isolation infrared spectroscopy is similar to those previously reported.⁹ Briefly, the Nd:YAG laser fundamental (1064 nm, 10 Hz repetition rate with 10 ns pulse width) was focused on the rotating Cd target. The laser-ablated Cd atoms were codeposited with CO in excess argon onto a CsI window cooled normally to 7 K by means of a closed-cycle helium refrigerator. Typically, 1–5 mJ/pulse laser power was used. Carbon monoxide (99.95% CO), $^{13}\text{C}^{16}\text{O}$ (99%, [^{18}O] < 1%), and $^{12}\text{C}^{18}\text{O}$ (99%) were used to prepare the CO/Ar mixtures. In general, matrix samples were deposited for 1–2 h with a typical rate of 2–4 mmol/h. After sample deposition, IR spectra were recorded on a BIO-RAD FTS-6000e spectrometer at 0.5 cm^{-1} resolution using a liquid nitrogen cooled HgCdTe (MCT) detector for the spectral range of 5000–

* To whom correspondence should be addressed at AIST. E-mail: q.xu@aist.go.jp.

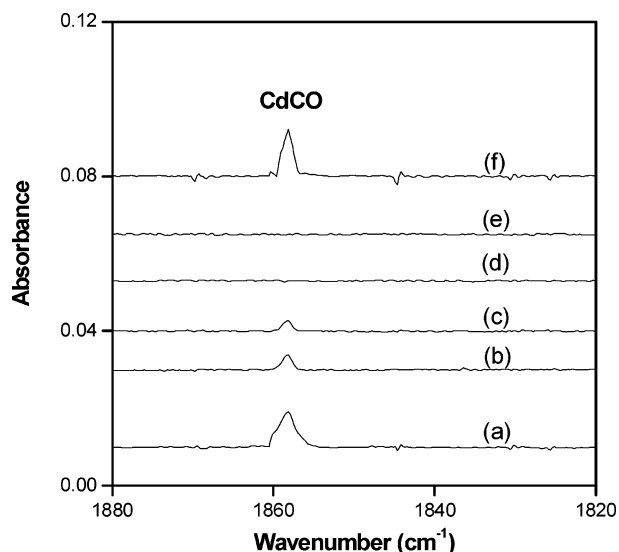


Figure 1. IR spectra in the 1880–1820 cm^{-1} region for laser-ablated Cd atoms codeposited with 0.5% CO in argon at 7 K: (a) 60 min of sample deposition, (b) after annealing to 25 K, (c) after annealing to 30 K, (d) after 20 min of broad-band irradiation, (e) after annealing to 34 K, and (f) doping with 0.05% CCl_4 , after 60 min of sample deposition.

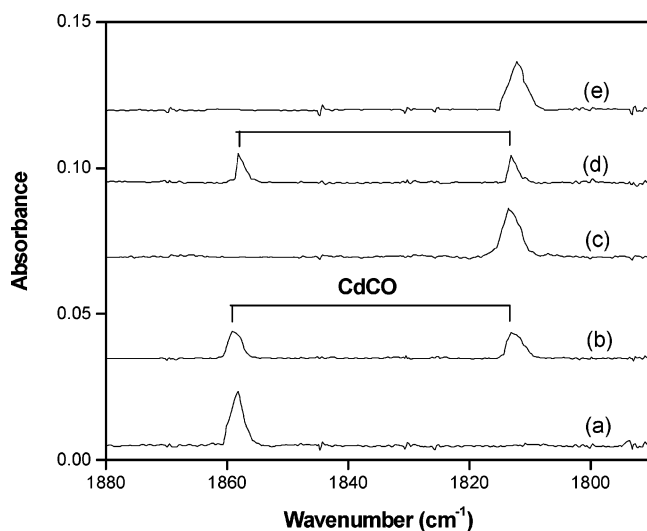


Figure 2. IR spectra in the 1880–1800 cm^{-1} region for laser-ablated Cd atoms codeposited with isotopic CO in Ar for 60 min of sample deposition at 7 K: (a) 0.5% $^{12}\text{C}^{16}\text{O}$, (b) 0.25% $^{12}\text{C}^{16}\text{O}$ + 0.25% $^{13}\text{C}^{16}\text{O}$, (c) 0.5% $^{13}\text{C}^{16}\text{O}$, (d) 0.25% $^{12}\text{C}^{16}\text{O}$ + 0.25% $^{12}\text{C}^{18}\text{O}$, and (e) 0.5% $^{12}\text{C}^{18}\text{O}$.

400 cm^{-1} . Samples were annealed at different temperatures and subjected to broad-band irradiation ($\lambda > 250$ nm) using a high-pressure mercury arc lamp (Ushio, 100 W).

Quantum chemical calculations were performed to predict the structures and vibrational frequencies of the observed reaction products using the Gaussian 03 program.¹⁰ The BP86 and B3LYP density functional methods were used.¹¹ The D95* and 6-311++G(3df,3pd) basis sets were used for C and O atoms,¹² and the Los Alamos ECP plus DZ (LANL2DZ) basis

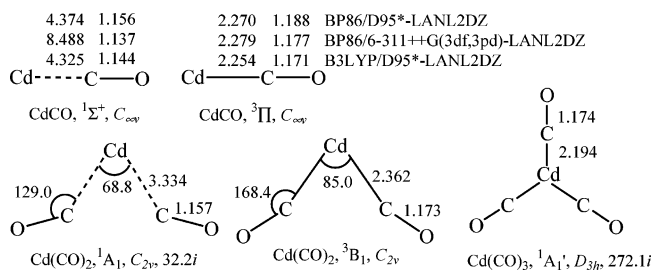


Figure 3. Optimized structures (bond lengths in angstroms, bond angles in degrees), electronic ground states, and point groups of the $\text{Cd}(\text{CO})_n$ ($n = 1-3$) molecules. For $\text{Cd}(\text{CO})_n$ ($n = 2, 3$), the calculations have been performed at the BP86/D95*-LANL2DZ level and the letter “i” denotes the imaginary frequency (cm^{-1}).

set was used for Cd atoms.¹³ Geometries were fully optimized, and vibrational frequencies were calculated with analytical second derivatives. A natural bond orbital (NBO) analysis¹⁴ was carried out at the stationary points to give further insight into their bonding properties.

Results and Discussion

Experiments have been done with carbon monoxide concentrations ranging from 0.02% to 1.0% in excess argon. Typical infrared spectra for the reactions of laser-ablated Cd atoms with CO molecules in excess argon in the selected regions are illustrated in Figures 1 and 2, and the absorption bands in different isotopic experiments are listed in Table 1. The stepwise annealing and photolysis behavior of the product absorptions is also shown in the figures and will be discussed below. Experiments were also done with doping CCl_4 of different concentrations serving as an electron scavenger in solid argon.

Quantum chemical calculations have been carried out for the possible isomers and electronic states of the potential product molecules. Figure 3 shows the optimized structures of the reaction products. Molecular orbital pictures of triplet CdCO, showing the highest occupied molecular orbitals down to the fourth valence molecular orbital from the HOMO, are plotted in Figure 4. Figure 5 schematically shows the energy levels of the valence 4d, 4s, and 4p orbitals of the Cd atom and those of the lone-pair electrons of CO and its vacant π^* orbitals compared with those of the Cu, Ag, and Zn atoms. The natural electron configuration of the CdCO molecule is listed in Table 2. To address the bonding characteristics, we report the results from NBO analysis for the CdCO molecule in Table 3. Meanwhile, the calculations for the $\text{Cd}(\text{CO})_n$ ($n = 2, 3$) species have also been considered at the same theory level, and salient results are shown in Figure 3.

CdCO. The feature in the C–O stretching region at 1858.2 cm^{-1} (Table 1 and Figure 1) has been observed after sample deposition. This band sharply decreases on annealing, disappears after broad-band irradiation, and does not recover after further annealing. The 1858.2 cm^{-1} band shifts to 1813.5 cm^{-1} with $^{13}\text{C}^{16}\text{O}$ and to 1812.3 cm^{-1} with $^{12}\text{C}^{18}\text{O}$, exhibiting isotopic frequency ratios ($^{12}\text{C}^{16}\text{O}/^{13}\text{C}^{16}\text{O}$, 1.0246; $^{12}\text{C}^{16}\text{O}/^{12}\text{C}^{18}\text{O}$, 1.0253) characteristic of C–O stretching vibrations. The mixed $^{12}\text{C}^{16}\text{O} + ^{13}\text{C}^{16}\text{O}$ and $^{12}\text{C}^{16}\text{O} + ^{12}\text{C}^{18}\text{O}$ isotopic

TABLE 1: Observed and Calculated Vibrational Frequencies (cm^{-1}) and Isotopic Frequency Ratios for the Triplet CdCO Molecule

	$^{12}\text{C}^{16}\text{O}$	$^{13}\text{C}^{16}\text{O}$	$^{12}\text{C}^{18}\text{O}$	$^{12}\text{C}/^{13}\text{C}$	$^{16}\text{O}/^{18}\text{O}$
observed	1858.2	1813.5	1812.3	1.0246	1.0253
BP86/D95*-LANL2DZ	1860.5	1818.1	1817.1	1.0233	1.0239
BP86/6-311++G(3df,3pd)-LANL2DZ	1863.0	1820.7	1819.3	1.0232	1.0240
B3LYP/D95*-LANL2DZ	1905.1	1861.8	1860.4	1.0233	1.0240

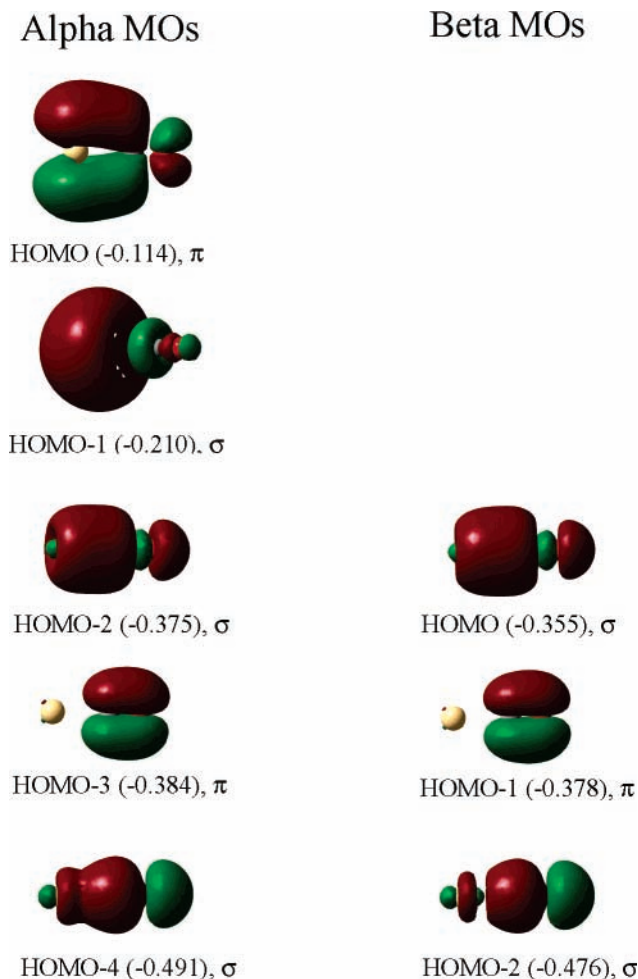


Figure 4. Molecular orbital pictures of triplet CdCO, showing the highest occupied molecular orbitals down to the fourth valence molecular orbital from the HOMO. α HOMO - 3 and β HOMO - 1 each consist of one degenerate pair, and only one of them is plotted. The unit of orbital energy is hartrees (in parentheses).

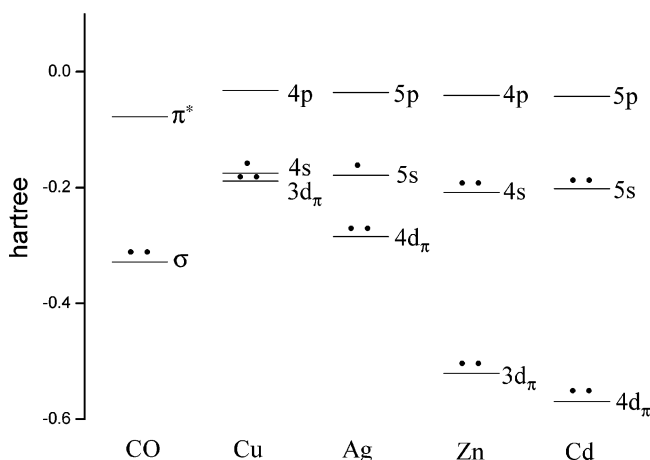


Figure 5. Energy levels of the valence ($n - 1$)d, ns , and np orbitals of the Cu, Ag, Zn, and Cd atoms and those of the lone-pair electrons of CO and its vacant π^* orbitals.

spectra (Figure 2) only provide the sum of pure isotopic bands, which indicates a monocarbonyl molecule.¹⁵ As can be seen in Figure 1, doping with CCl_4 has no effect on this band, suggesting that the product is neutral.^{3a} The 1858.2 cm^{-1} band is therefore assigned to the C–O stretching vibration of the neutral cadmium monocarbonyl, CdCO.

The density functional theory (DFT) calculations lend strong support for the assignment. At the BP86/D95*-LANL2DZ level, the C–O stretching vibrational frequency ($\nu_{\text{C-O}}$) and $R_{\text{Cd-C}}$ of the singlet CdCO are predicted to be 2094.0 cm^{-1} and 4.374 \AA (Figure 3), respectively, and the singlet CdCO lies 55 kcal/mol lower in energy than the triplet one ($\nu_{\text{C-O}} = 1860.5 \text{ cm}^{-1}$, $R_{\text{Cd-C}} = 2.270 \text{ \AA}$), indicating that the triplet state drives the Cd–C bond distance closer. It is reasonable that the triplet excimer could be trapped instead of the lower energy singlet CdCO species. The other vibrational modes of the triplet CdCO are calculated to be 283.2 (intensity 7.5 km/mol), 233.8 (6.0), and 153.0 (0.8) cm^{-1} , which are beyond the present spectral range of $5000\text{--}400 \text{ cm}^{-1}$. At the BP86/6-311++G(3df,3pd)-LANL2DZ level, the singlet CdCO (2126.4 cm^{-1} , 8.488 \AA) is about 57 kcal/mol lower in energy than the triplet one (1863.0 cm^{-1} , 2.279 \AA). At the B3LYP/D95*-LANL2DZ level, the singlet (2185.1 cm^{-1} , 4.325 \AA) is about 60 kcal/mol lower in energy than the triplet (1905.1 cm^{-1} , 2.254 \AA). The calculated $\nu_{\text{C-O}}$ values of the triplet CdCO at the BP86/D95*-LANL2DZ (1860.5 cm^{-1} , Table 1) and BP86/6-311++G(3df,3pd)-LANL2DZ (1863.0 cm^{-1}) levels show very good scale factors (the ratios of the observed frequency to the calculated frequency) of 0.999 and 0.997 , respectively. Equally importantly, the calculated $^{12}\text{C}^{16}\text{O}/^{13}\text{C}^{16}\text{O}$ and $^{12}\text{C}^{16}\text{O}/^{12}\text{C}^{18}\text{O}$ isotopic frequency ratios of 1.0233 (1.0232) and 1.0239 (1.0240) are in accord with the experimental observations, 1.0246 and 1.0253 , respectively. These excellent agreements substantiate the identification of this triplet cadmium monocarbonyl, CdCO, from the matrix IR spectra. This excimer state of CdCO conforms to its weak thermal stability; namely, the intensity of CdCO absorption decreases upon annealing and disappears after broad-band irradiation (Figure 1). The CdCO excimer may be formed during the codeposition of CO with the “hot” Cd atoms ablated by a pulse laser and has fortunately been captured by the matrix isolation technique. As outlined in Scheme 1, the formation of the triplet CdCO from Cd (^3P) and CO is exothermic (-32 kcal/mol), which is more favorable than the endothermic formation of the singlet CdCO from Cd (^1S) with CO ($+1 \text{ kcal/mol}$). Also, the CdCO excimer readily decomposes to the separate Cd (^1S) atom and CO molecule upon annealing (-56 kcal/mol), which does not favor the further addition of CO to form higher cadmium carbonyls.

Hereafter, mainly BP86/D95*-LANL2DZ results are presented for discussion. The present DFT calculations predict that the triplet cadmium dicarbonyl, Cd(CO)₂, has a C_{2v} symmetry with an $R_{\text{Cd-C}}$ of 2.362 \AA (Figure 3), and the triplet Cd(CO)₂ lies 40 kcal/mol higher in energy than the singlet one with one imaginary frequency at 32.2 cm^{-1} . Similarly, the cadmium tricarbonyl, Cd(CO)₃, is predicted to have a $^1\text{A}_1'$ state with D_{3h} symmetry, and the geometry optimization procedures starting with C_1 , C_{2v} , and C_{3h} symmetry all result in structures closer to D_{3h} symmetry, which all have one imaginary frequency (272.1 cm^{-1}). The triplet Cd(CO)₃ molecule exhibits no geometry convergence. Thus, there is no indication for a strong Cd–CO interaction leading to the formation of Cd(CO)₃, consistent with the absence of this species in the present matrix IR spectra. This feature is different from the reactions of Zn atoms with CO, by which the Zn(CO)₃ molecule was observed but no formation of Zn(CO)_{*n*} ($n = 1, 2$).⁶

In contrast, the natural charge of the cadmium atom in CdCO is $+0.56$, exhibiting a large charge transfer from Cd to CO and therefore sharply lowering the CO stretching frequency. It is noted that the HOMO–LUMO gap of CdCO (3.74 kcal/mol) is lower than that of Cd(CO)₂ (67.22 kcal/mol) and Cd(CO)₃

TABLE 2: Natural Electron Configuration of the Triplet CdCO Molecule Calculated at the BP86/D95*-LANL2DZ Level

atom	natural electron configuration
Cd	[core]5s(1.11)4d(9.99)5p(0.34)
C	[core]2s(1.51)2p(2.51)3s(0.03)3p(0.05)
O	[core]2s(1.74)2p(4.70)3p(0.01)3d(0.02)

atom	α spin orbitals	β spin orbitals
Cd	[core]5s(0.96)4d(5.00)5p(0.34)	[core]5s(0.15)4d(4.99)
C	[core]2s(0.81)2p(1.53)3s(0.02)3p(0.04)	[core]2s(0.70)2p(0.99)3s(0.01)3p(0.01)
O	[core]2s(0.87)2p(2.43)3p(0.01)3d(0.01)	[core]2s(0.87)2p(2.27)3d(0.01)

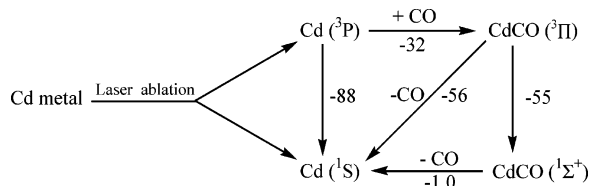
TABLE 3: Natural Bond Orbital Analysis Results of the Triplet CdCO Molecule Calculated at the BP86/D95*-LANL2DZ Level^a

bond	spin	type	Cd (%)				C (%)			
			100 C _A ²	s	p	d	100 C _A ²	s	p	d
Cd–C	α	π	23.70	0.00	99.72	0.28	76.30	0.00	99.99	0.01
Cd–C	β	σ	14.11	98.52	1.06	0.43	85.89	58.71	41.28	0.01

bond	spin	type	C (%)				O (%)			
			100 C _A ²	s	p	d	100 C _A ²	s	p	d
C–O	α	π	28.51	0.00	99.77	0.23	71.49	0.00	99.69	0.31
C–O	α	σ	30.02	28.39	71.44	0.17	69.98	42.39	57.14	0.47
C–O	β	π	27.19	0.00	99.73	0.27	72.81	0.00	99.68	0.32
C–O	β	σ	30.77	42.82	56.99	0.19	69.23	41.49	58.04	0.48

^a C_A is the polarization coefficient.

SCHEME 1: Reaction Mechanism of Laser-Ablated Cadmium Atoms with Carbon Monoxide in Solid Argon^a



^a A negative value of energy (kcal/mol) denotes that the reaction is exothermic.

(13.35 kcal/mol). The formation of CdCO from the reactions of CO with the Cd (¹S) atom is endothermic (+55.49 kcal/mol), but exothermic (−32.20 kcal/mol) with Cd (³P), implying that the formation of CdCO involves the electronic excitation of the Cd atom to the ³P state (vide infra).

Bonding Mechanism. The natural electron configuration of Cd in CdCO is [core]5s(1.11)4d(9.99)5p(0.34) (Table 2), suggesting that the formation of CdCO involves 5s → 5p promotion of the Cd atom. As illustrated in Figure 4, the α spin HOMO is the Cd–C π bonding orbital (also shown in Table 3), which comprises the Cd 5p orbital → CO π^* back-donation, satisfying the frontier molecular orbital (FMO) theory.¹⁶ This promotion increases the Cd–CO bonding by decreasing the σ repulsion and significantly increasing the Cd 5p orbital → CO π^* back-donation. The contribution for the formation of the Cd–C bond is primarily from the interaction between Cd 5p (99.72%) and C 2p (99.99%) orbitals (Table 3). The α spin HOMO − 1 is largely Cd 5s in character and is nonbonding. The α spin HOMO − 2 is a Cd–C–O σ -type bonding orbital, similar to the β spin HOMO. The α spin HOMO − 3 and HOMO − 4 mainly depict the enhanced π -type and depressed σ -type C–O bonds, respectively, and the same are the corresponding β spin molecular orbitals (Table 3). Furthermore, the states of $\tilde{X}^1\Sigma^+$, $\tilde{A}^1\Pi$, and $\tilde{a}^3\Pi$ can be derived from the two nominal configurations (... σ^2 and ... $\sigma^1\pi^1$) of this linear molecule. This regular $\tilde{a}^3\Pi$ state is indeed metastable and presumably can be trapped in a matrix because there is a

barrier to rearrangement. The molecule is on a triplet surface that can cross via the $\tilde{a}^3\Pi_0^+$ spin component over to the singlet $\tilde{X}^1\Sigma^+$ surface, but this rearrangement must have a barrier. In contrast, a similar rearrangement for ZnCO might have a lower barrier, and then it is more difficult to capture the triplet ZnCO.

As shown in Figure 5, the metal ($n - 1$) d_π of the Ag, Zn, and Cd atoms and CO π^* levels are farther apart than in the Cu atom. Thus, the $d_\pi \rightarrow \pi^*$ donation is expected to be energetically unfavorable for the formation of MCO (M = Ag, Zn, Cd).^{3–6} Interestingly, the zinc tricarbonyl, Zn(CO)₃, has been recently observed from the reaction of laser-ablated Zn atoms with CO in excess argon, whereas the zinc mono- and dicarbonyls, Zn(CO)_n ($n = 1, 2$), have not been observed.⁶ The 4s → 4p promotion of the Zn atom has been found in the formation of Zn(CO)₃, which increases the Zn–CO bonding by decreasing the σ repulsion and significantly increasing the Zn 4sp hybrid orbitals → CO π^* back-donation. The quenching from the Zn ³P atom to ¹S in Zn(CO)₃ corresponds to the stabilization by the overlapped C₃ orbitals, and the sp² hybrid orbitals of Zn atom are favorable to bond three CO molecules. For CdCO, the aforementioned 5s → 5p promotion of the Cd atom (Table 3) is primarily responsible for its metastability, which increases the Cd–CO bonding by decreasing the σ repulsion and significantly increasing the Cd 5p orbital → CO π^* back-donation. The $ns \rightarrow np$ excitation energy of the Cd atom (100.07 kcal/mol) is slightly lower than that of the Zn atom (111.28 kcal/mol). In contrast, it has been found that ³P excited metal atoms react with H₂ in the matrix to form the group 12 hydride molecules.^{3b,17} To form the monometal hydride species, CH₃MH (M = Zn, Cd, Hg), excitation to the ³P metal atom state was also required to promote insertion into a methane molecule.¹⁷ Along with the aforementioned reports,^{3b,17,18} the present finding shows that a number of novel species difficult to form from the reactions of ground-state metals are generated using excitation methods such as laser ablation and irradiation by a microwave-powered reactive resonance lamp.

Conclusions

Reactions of laser-ablated cadmium atoms with carbon monoxide molecules in solid argon have been studied using matrix isolation infrared spectroscopy. The absorption at 1858.2 cm^{-1} is assigned to the C–O stretching of the CdCO molecule on the basis of isotopic substitution. Density functional theory calculations have been performed on the cadmium carbonyls $\text{Cd}(\text{CO})_n$ ($n = 1-3$), which lend strong support to the experimental assignments of the infrared spectra. It is predicted that the CdCO molecule is a linear triplet molecule and its formation involves $\text{Cd } 5s \rightarrow 5p$ promotion. This promotion increases the Cd–CO bonding by decreasing the σ repulsion and increasing the Cd $5p$ orbital \rightarrow CO π^* back-donation. The absence of cadmium di- and tricarbonyls, $\text{Cd}(\text{CO})_n$ ($n = 2, 3$), has also been discussed in some detail.

Acknowledgment. We thank Prof. Mingfei Zhou for helpful discussion and the reviewers for valuable comments and suggestions. This work was supported by a Grant-in-Aid for Scientific Research (B) (Grant No. 17350012) from the Ministry of Education, Culture, Sports, Science and Technology (MEXT) of Japan and by the Marubun Research Promotion Foundation. L.J. thanks MEXT of Japan and Kobe University for an Honors Scholarship.

References and Notes

- (1) Cotton, F. A.; Wilkinson, G.; Murillo, C. A.; Bochmann, M. *Advanced Inorganic Chemistry*, 6th ed.; Wiley: New York, 1999.
- (2) Blyholder, G. J. *Phys. Chem.* **1964**, *68*, 2772.
- (3) (a) Zhou, M. F.; Andrews, L.; Bauschlicher, C. W., Jr. *Chem. Rev.* **2001**, *101*, 1931. (b) Himmel, H. J.; Downs, A. J.; Greene, T. M. *Chem. Rev.* **2002**, *102*, 4191 and references therein.
- (4) Huber, H.; Kunding, E. P.; Moskovits, M.; Ozin, G. A. *J. Am. Chem. Soc.* **1975**, *97*, 2097. Kasai, P. H.; Jones, P. M. *J. Am. Chem. Soc.* **1985**, *107*, 813. Chemier, J. H. B.; Hampson, C. A.; Howard, J. A.; Mile, B. *J. Phys. Chem.* **1989**, *93*, 114. Blitz, M. A.; Mitchell, S. A.; Hackett, P. A. *J. Phys. Chem.* **1991**, *95*, 8719. Zhou, M. F.; Andrews, L. *J. Chem. Phys.* **1999**, *111*, 4548.
- (5) McIntosh, D.; Ozin, G. A. *J. Am. Chem. Soc.* **1976**, *98*, 3167. Kasai, P. H.; Jones, P. M. *J. Phys. Chem.* **1985**, *89*, 1147. Kasai, P. H.; Jones, P. M. *J. Am. Chem. Soc.* **1985**, *107*, 6385. Marian, C. M. *Chem. Phys. Lett.* **1993**, *215*, 582. Liang, B.; Andrews, L. *J. Phys. Chem. A* **2000**, *104*, 9156.
- (6) Jiang, L.; Xu, Q. *J. Am. Chem. Soc.* **2005**, *127*, 8906.
- (7) Li, J.; Bursten, B. E.; Liang, B.; Andrews, L. *Science* **2002**, *295*, 2242. Andrews, L.; Wang, X. *Science* **2003**, *299*, 2049.
- (8) Zhou, M. F.; Tsumori, N.; Li, Z.; Fan, K.; Andrews, L.; Xu, Q. *J. Am. Chem. Soc.* **2002**, *124*, 12936. Zhou, M. F.; Xu, Q.; Wang, Z.; von Ragué Schleyer, P. *J. Am. Chem. Soc.* **2002**, *124*, 14854. Jiang, L.; Xu, Q. *J. Am. Chem. Soc.* **2005**, *127*, 42.
- (9) Burkholder, T. R.; Andrews, L. *J. Chem. Phys.* **1991**, *95*, 8697. Zhou, M. F.; Tsumori, N.; Andrews, L.; Xu, Q. *J. Phys. Chem. A* **2003**, *107*, 2458. Jiang, L.; Xu, Q. *J. Chem. Phys.* **2005**, *122*, 034505.
- (10) Frisch, M. J.; Trucks, G. W.; Schlegel, H. B.; Scuseria, G. E.; Robb, M. A.; Cheeseman, J. R.; Montgomery, J. A., Jr.; Vreven, T.; Kudin, K. N.; Burant, J. C.; Millam, J. M.; Iyengar, S. S.; Tomasi, J.; Barone, V.; Mennucci, B.; Cossi, M.; Scalmani, G.; Rega, N.; Petersson, G. A.; Nakatsuji, H.; Hada, M.; Ehara, M.; Toyota, K.; Fukuda, R.; Hasegawa, J.; Ishida, M.; Nakajima, T.; Honda, Y.; Kitao, O.; Nakai, H.; Klene, M.; Li, X.; Knox, J. E.; Hratchian, H. P.; Cross, J. B.; Adamo, C.; Jaramillo, J.; Gomperts, R.; Stratmann, R. E.; Yazyev, O.; Austin, A. J.; Cammi, R.; Pomelli, C.; Ochterski, J. W.; Ayala, P. Y.; Morokuma, K.; Voth, G. A.; Salvador, P.; Dannenberg, J. J.; Zakrzewski, V. G.; Dapprich, S.; Daniels, A. D.; Strain, M. C.; Farkas, O.; Malick, D. K.; Rabuck, A. D.; Raghavachari, K.; Foresman, J. B.; Ortiz, J. V.; Cui, Q.; Baboul, A. G.; Clifford, S.; Cioslowski, J.; Stefanov, B. B.; Liu, G.; Liashenko, A.; Piskorz, P.; Komaromi, I.; Martin, R. L.; Fox, D. J.; Keith, T.; Al-Laham, M. A.; Peng, C. Y.; Nanayakkara, A.; Challacombe, M.; Gill, P. M. W.; Johnson, B.; Chen, W.; Wong, M. W.; Gonzalez, C.; Pople, J. A. *Gaussian 03*, revision B.04; Gaussian, Inc.: Pittsburgh, PA, 2003.
- (11) Becke, A. D. *Phys. Rev. A* **1988**, *38*, 3098. Perdew, J. P. *Phys. Rev. B* **1986**, *33*, 8822. Lee, C.; Yang, E.; Parr, R. G. *Phys. Rev. B* **1988**, *37*, 785. Becke, A. D. *J. Chem. Phys.* **1993**, *98*, 5648.
- (12) Dunning, T. H., Jr.; Hay, P. J. In *Modern Theoretical Chemistry*; Schaefer, H. F., III, Ed.; Plenum: New York, 1976; Vol. 3, p 1. McLean, A. D.; Chandler, G. S. *J. Chem. Phys.* **1980**, *72*, 5639. Krishnan, R.; Binkley, J. S.; Seeger, R.; Pople, J. A. *J. Chem. Phys.* **1980**, *72*, 650. Frisch, M. J.; Pople, J. A.; Binkley, J. S. *J. Chem. Phys.* **1984**, *80*, 3265.
- (13) Hay, P. J.; Wadt, W. R. *J. Chem. Phys.* **1985**, *82*, 299.
- (14) Glendening, E. D.; Reed, A. E.; Carpenter, J. E.; Weinhold, F. *NBO*, version 3.1.
- (15) Darling, J. H.; Ogden, J. S. *J. Chem. Soc., Dalton Trans.* **1972**, 2496.
- (16) Fukui, K. *Acc. Chem. Res.* **1971**, *4*, 57. Woodward, R. B.; Hoffmann, R. *The Conservation of Orbital Symmetry*; Chemie: Weinheim, Germany, 1970.
- (17) Greene, T. M.; Brown, W.; Andrews, L.; Downs, A. J.; Chertihin, G. V.; Runeberg, N.; Pyykkö, P. *J. Phys. Chem.* **1995**, *99*, 7925. Breckenridge, W. H.; Wang, J. H. *J. Chem. Phys.* **1987**, *87*, 2630. Wang, X.; Andrews, L. *J. Phys. Chem. A* **2004**, *108*, 11006. Wang, X.; Andrews, L. *Inorg. Chem.* **2004**, *43*, 7146.
- (18) Greene, T. M.; Andrews, L.; Downs, A. J. *J. Am. Chem. Soc.* **1995**, *117*, 8180.